Interaction Note 172

April 1974

SHIELDING EFFECTIVENESS OF BRAIDED WIRE SHIELDS

by

E. F. Vance
Stanford Research Institute
Menlo Park, California

ABSTRACT

An analysis of the shielding effectiveness of braided-wire shields is made using the parameters of the woven wire and the theory of electromagnetic coupling through small irises. The coupling through the rhombic-shaped holes in the braid is approximated by using the electric and magnetic polarizabilities of elliptical holes of the same width and length as the rhombus. The analysis is concentrated on the transfer impedance and the mutual capacitance of the shield. The transfer impedance is calculated and plotted for several shields of different optical coverages. The variation of mutual capacitance and mutual inductance with the weave angle of the braid are examined, and the transfer characteristics of two-layer shields is analyzed.

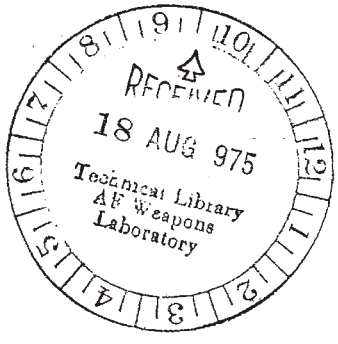

I INTRODUCTION

This note is concerned with the analysis of braided-wire shields of the type commonly used in RF transmission lines and in shielded multiconductor cables for electronic systems. The analysis is based on the theory of coupling through electrically small irises and follows the procedures developed by Marcuvitz and Kaden.[1,2] The small-iris theory is then adapted to the single-layer braided shield so that the transfer impedance of the braided shield can be expressed in terms of physical parameters of the braid such as wire size, number of wires per carrier, number of carriers, and weave angle (or picks). Finally, this analysis is carried further to develop the transfer impedance and admittance for double-braided shields. These transfer characteristics of a typical high-coverage braided shield and of a double-braided shield, each layer of which has the same coverage, are calculated for comparison. The expressions for the transfer impedance and admittance and shield parameters are arranged in such a manner that the effect of varying such parameters as shield transparency (or coverage), wire size, weave angle, etc., can be assessed.

The transfer impedance of a shield is one measure of the effectiveness of the shield. It is a property of the shield alone, and is therefore independent of the type of core conductors inside the shield and of the type of loads between the ends of these core conductors and the shield. In its most general form, the transfer impedance is defined as

$$Z_T = \frac{1}{I} \frac{dV}{dx} \qquad (1)$$

where I is the total current flowing in the shield, and dV/dx is the change in voltage generated by this current along the transmission line formed by the shield and in imaginary perfectly conducting filament enclosed by the shield. (For a cylindrical shield of circular cross section the perfectly conducting filament may be visualized as lying along the axis of the cylinder.) For solid-walled metal shields in which the only fields that appear inside the shield are those that diffuse through the metal, dV/dx = E, where E is the longitudinal electric field along the inside surface of the shield, and the transfer impedance can be written

$$Z_T = \frac{E}{I} \quad . \tag{2}$$

Shields that permit the exterior fields to penetrate through holes, cracks, etc., in the metal wall are characterized by mutual-coupling components as well as the diffusion components, so that the more general definition of transfer impedance given in Eq. (1) is required.

The transfer impedance of a shield can be measured in the laboratory by producing a known current in the shield (with external fields) and measuring the voltage developed along 1 meter of shield between a small wire inside the shield and the wall of the shield. This experiment is shown schematically in Figure 1, where the shield current is developed by making the shield the center conductor of a coaxial transmission line. The voltage developed along an electrically short length ℓ inside the shield is measured by connecting a wire to one end of the shield, running it through the shield, and measuring the voltage developed between the wire and the shield at the opposite end of the shield. The transfer impedance is then

$$Z_T = \frac{V}{\ell I} \quad . \tag{3}$$

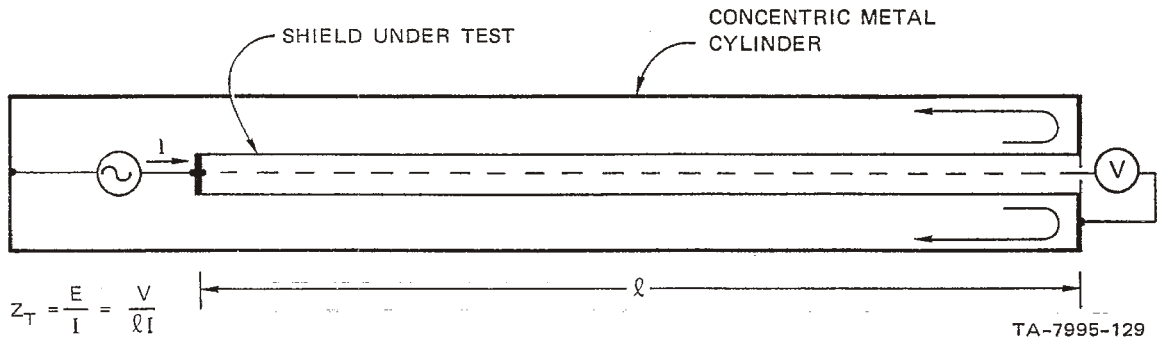

FIGURE 1 SCHEMATIC DIAGRAM OF TRANSFER IMPEDANCE MEASUREMENT CIRCUIT

To apply the transfer impedance to cable analysis in which the currents and voltages developed on conductors inside the shields are to be determined, given the shield current I, the transfer impedance and shield current are treated as a distributed source in what is otherwise a classical transmission-line analysis. An element of the transmission line of length dx is illustrated in Figure 2(a) with the element of distributed voltage source $Z_T I_o dx$. The differential equations for the common-mode current and voltage on the internal conductors are

$$\frac{\partial V}{\partial x} + Z I = Z_T I \tag{4}$$

$$\frac{\partial I}{\partial x} + YV = 0 \tag{5}$$

These can be combined and written as second-order differential equations in the current and voltage as

$$\frac{\partial^2 I}{\partial x^2} - \gamma^2 I = - YZ_T I_o \tag{6}$$

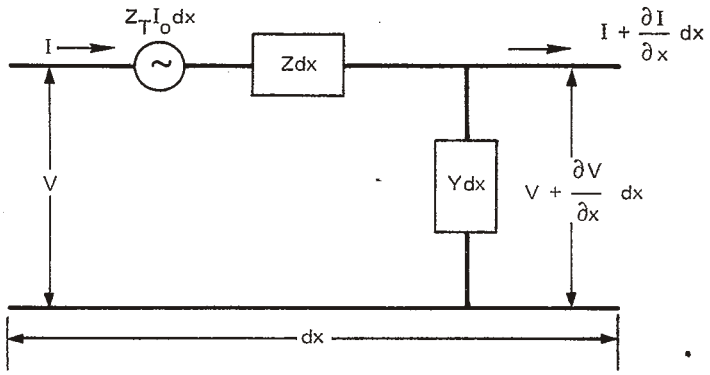

(a) DISTRIBUTED SOURCE $I_o Z_T$

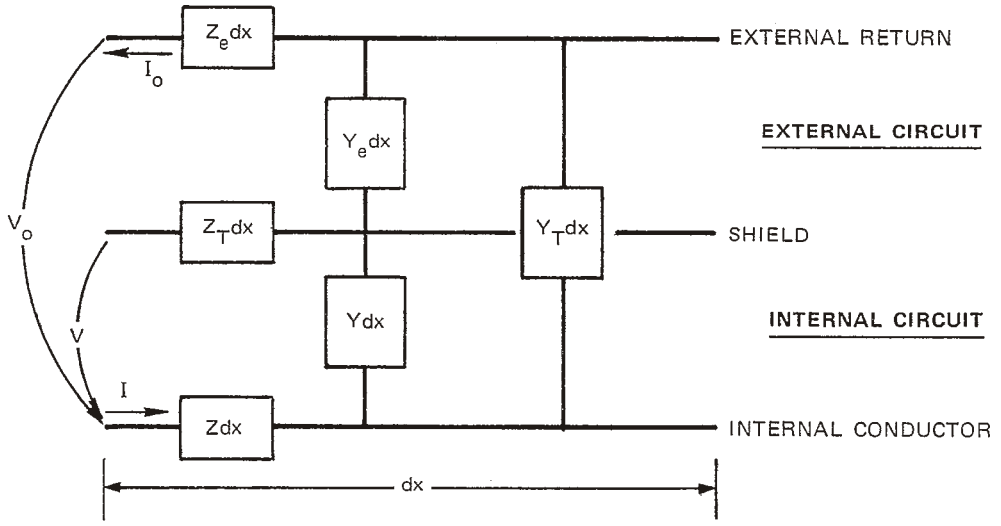

(b) COUPLED LINE SHOWING TRANSFER IMPEDANCE Z_T AND ADMITTANCE Y_T

TA-7995-220R

FIGURE 2 TRANSMISSION LINE MODELS INCORPORATING THE TRANSFER IMPEDANCE AND THE TRANSFER ADMITTANCE

$$\frac{\partial^2 V}{\partial x^2} - \gamma^2 V = Z_T \frac{\partial I}{\partial x} \quad ; \tag{7}$$

where $\gamma^2 = YZ$. These equations are identical to the classical transmission-line equations except for the terms on the right containing Z_T and I. These equations can be solved, subject to the applicable boundary conditions for the common-mode voltage V and current I_i at any point along the cable. (If the cable is to be modeled as a chain of lumped-element sections, the infinitesimal length dx in Figure 2(a) is replaced by a finite length ℓ, and classical circuit analysis techniques are applied.)

In addition to the coupling produced by penetration of the magnetic field through the openings in the shield, there may also be electric coupling produced by an electric field, which would otherwise terminate on the outer surface of the shield, penetrating through the holes in the shield and terminating on the inner conductors. Coupling of this form can be represented by a transfer admittance Y_T between the return path for the shield current and the inner conductors as illustrated in Figure 2(b). This transfer admittance is the susceptance per unit length between the inner conductor and the shield return-current path. As implied in Figure 2(b), an analysis of the effects of electric coupling (and, indeed, the specification of Y_T) requires that the external circuit of the shield current be considered, as well as the internal circuit of the shielded conductors. The transfer admittance can be measured in the circuit of Figure 1 if the outer structure is open-circuited at the right end (so that no current flows in the shield) and the short-circuit current, instead of the open-circuit voltage, is measured.

The derivation of the transfer admittance of a hole in a shield with a concentric return is also given by Kaden. This derivation develops

the equivalent electric-dipole moment associated with an electrically small iris and the charge induced on the internal conductors by this dipole moment. The analysis yields a mutual capacitance C_{12} between the internal conductors and the shield return path associated with the hole (iris) in the shield. The transfer admittance associated with holes is then $Y_T = j\omega C_{12}$.

When the transfer admittance Y_T is included the increment of transmission line contains a shunt current source $V_o Y_T$ as well as a series voltage source $I_o Z_T$. The equivalent circuit of the increment of transmission line containing both sources is shown in Figure 3. Notice in

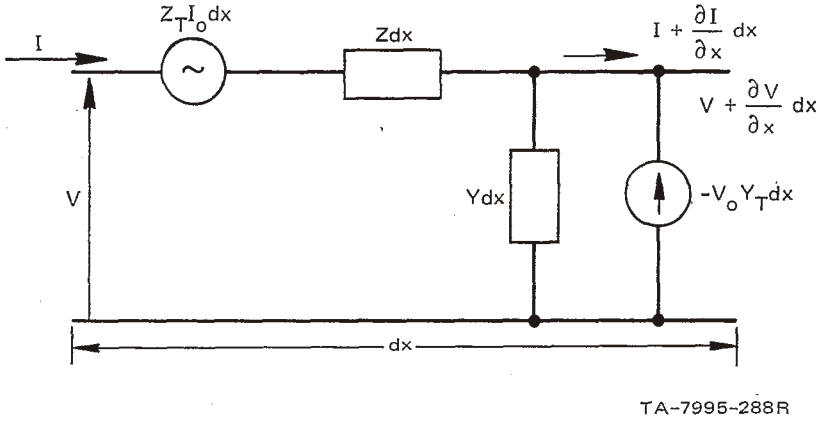

FIGURE 3 EQUIVALENT CIRCUIT FOR THE INTERNAL CIRCUIT WHEN BOTH THE TRANSFER IMPEDANCE AND THE TRANSFER ADMITTANCE ARE INCLUDED

Figure 2(b) that a positive voltage V_o causes current to flow out of the internal conductor through Y_T, so that the distributed current source is $J = - V_o Y_T$ in Figure 3. When only the current source $V_o Y_T$ in Figure 3 is considered, the differential equations for the internal current and voltage become

$$\frac{\partial V}{\partial x} + ZI = 0 \qquad (8)$$

$$\frac{\partial I}{\partial x} + YV = V_o Y_T \qquad (9)$$

which can be combined to give the second order equation

$$\frac{\partial^2 V}{\partial x^2} - \gamma^2 V = ZY_T V_o \quad . \qquad (10)$$

This expression is also similar to the classical transmission line equation except for the source term $V_o Y_T$.

II PERFORATED TUBULAR SHIELD

A. Transfer Impedance

The properties of leaky shields can be ascertained by studying the perforated tubular shield illustrated in Figure 4. The cylindrical tube with uniformly distributed circular holes is amenable to precise analytical treatment which can be used to study the coupling mechanisms and to clearly define the effect of shield coverage and hole size on shielding effectiveness.[1,2] The trends established for the perforated cylinder can then be used in the evaluation of more practical leaky shields such as braided or knitted shields, which do not yield to rigorous analytical treatment.

The transfer impedance of a perforated thin-walled shield consists of two parts--that due to diffusion through the metal, and that due to mutual coupling through the holes. The contribution of the diffusion is

$$Z_d = \frac{\gamma T}{\sigma A \sinh \gamma T} \qquad (11)$$

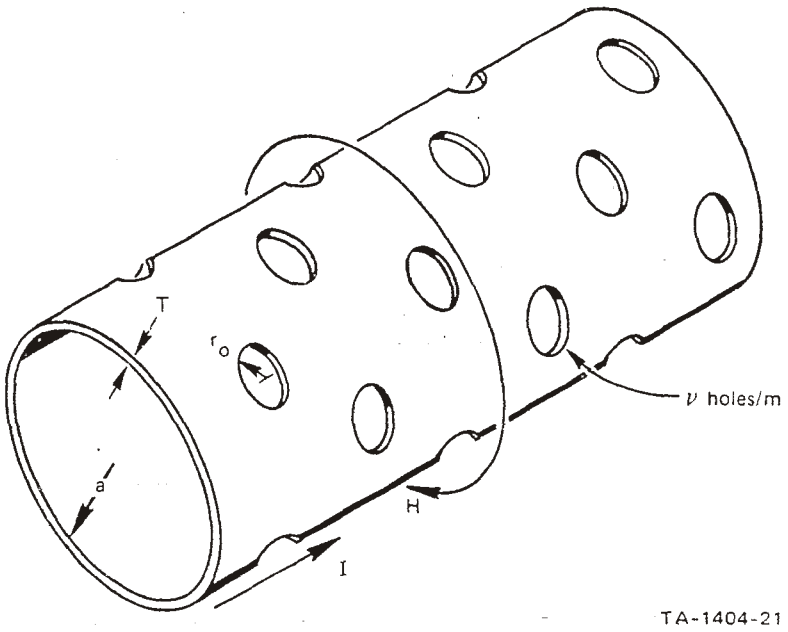

FIGURE 4 ILLUSTRATION OF A PERFORATED TUBULAR SHIELD

where A is the cross-section area of the metal in the tube, σ is the conductivity of the shield, T is its thickness, and γ is the propagation factor in the shield material. For a solid shield, $A = 2\pi aT$, but for a perforated shield containing υ uniformly distributed circular holes per unit length, each of radius r_o, the average cross-section area is

$$A = 2\pi aT - \upsilon\pi r_o^2 T$$

$$= 2\pi aT(1 - \tau) \qquad (12)$$

where τ is the transparency of the shield as defined by the ratio of the hole area to the total area of the surface of the shield:

$$\tau = \frac{\upsilon\pi r_o^2}{2\pi a} = \frac{\upsilon r_o^2}{2a} \qquad (13)$$

The diffusion component of the shield transfer impedance is thus

$$Z_d = \frac{\gamma}{2\pi a\sigma(1 - \tau)} \left(\frac{1}{\sinh \gamma T}\right). \tag{14}$$

The mutual-coupling component of the transfer impedance is produced by magnetic-field penetration through the holes in the shield and can be written

$$Z_m = j\omega \upsilon M_1 \tag{15}$$

where M_1 is the mutual coupling for one hole. The mutual coupling through a hole in a cylindrical shield of radius a depends on the size and shape of the hole and its orientation with respect to the current or magnetic field. The voltage induced inside a cylindrical shield by a magnetic field penetrating the hole is

$$V = j\omega \frac{\mu_o Hm}{2\pi a} \tag{16}$$

where H is the undisturbed magnetic field at the outside surface of the shield and m is the magnetic polarizability of the hole. The polarizability of a hole is the ratio of the effective dipole moment of the magnetic field penetrating the hole to the undisturbed magnetic field at the surface (i.e., $m = M_{eff}/\mu_o H$, where M_{eff} is the effective dipole moment of the magnetic field penetrating the hole). The polarizabilities of small holes have been derived for circles, ellipses, and narrow slits, and they have been measured for various other shapes.[3,4,5]

In terms of the current in the shield, the induced voltage is

$$V = j\omega\mu_o \frac{mI}{4\pi^2 a^2} \tag{17}$$

since

$$H = \frac{I}{2\pi a}$$

and the mutual inductance of one hole is thus

$$M_1 = \frac{\mu_o m}{4\pi^2 a^2} \quad . \tag{18}$$

The mutual-coupling term of the transfer impedance is thus

$$Z_m = j\omega\upsilon \frac{\mu_o m}{4\pi^2 a^2} \tag{19}$$

and the total transfer impedance is

$$Z_T = \frac{\gamma}{2\pi a\sigma(1 - \tau) \sinh \gamma T} + j\omega\upsilon \frac{\mu_o m}{4\pi^2 a^2} \quad . \tag{20}$$

The first term is identical to the transfer impedance of a solid shield except for the scalar factor $(1 - \tau)$, which increases the transfer impedance in proportion to the inverse of the shield coverage. The second term is a mutual-inductance term that depends on the number of openings υ in the shield and the polarizability m of each opening. The effect of the number and size of the openings can be made more apparent if a

particular hole shape, such as a circle, is assumed and the polarizability is evaluated. For a circle of radius r_o, the polarizability is

$$m = \frac{4r_o^3}{3} \tag{21}$$

and

$$j\omega\upsilon M_1 = j\omega\upsilon \frac{\mu_o r_o^3}{3\pi^2 a^2} = j\omega \frac{2\mu_o r_o \tau}{3\pi^2 a} \quad . \tag{22}$$

Thus it is seen that the mutual-coupling term depends not only on the transparency τ of the shield, but also on the size of the holes (r_o) by which this transparency is achieved. Thus a shield having a given transparency τ will be a more leaky shield if this transparency is caused by a few large holes than if it is caused by many small holes.

B. Transfer Admittance

By a similar analysis the transfer admittance relating the induced current per unit length J to the external voltage between the shield and its return path can be determined. The current per unit length induced in the internal conductor by the external electric field penetrating through the holes and terminating on the inner conductor is[1,2]

$$J = -V_o Y_T = -V_o j\omega C_{12}$$

$$= -V_o j\omega\upsilon \frac{pC_1C_2}{4\pi^2 a^2 \epsilon} \tag{23}$$

where p is the electric polarizability of the hole, C_1 is the capacitance per unit length between the inner conductor and the shield, and C_2 is the capacitance per unit length between the shield and its current return path. The voltage V_o is the voltage between the internal conductor and the shield current-return path [see Figure 2(b)]; for cable shields having no apparent current return path, the product $C_2 V_o$ can be replaced by an external charge per unit length Q_o.

For the circular hole of radius r_o, the electric polarizability is

$$p = \frac{2r_o^3}{3} \tag{24}$$

and the transfer admittance is

$$Y_T = j\omega\upsilon \frac{C_1 C_2 r_o^3}{6\pi^2 a^2 \varepsilon_o} = j\omega C_1 C_2 \frac{\tau r_o}{3\pi^2 a \varepsilon} \cdot \tag{25}$$

The transfer admittance is thus also proportional to the product of the coverage and the hole size. In addition, however, the transfer admittance depends on the external and internal characteristic impedances of the shield, as can be seen by substituting $C_1 = \frac{1}{vZ_o}$ and $C_2 = \frac{1}{v_e Z_{oe}}$:

$$Y_T = j\omega \frac{1}{vv_e Z_o Z_{oe}} \frac{\tau r_o}{3\pi^2 a \varepsilon} \cdot \tag{26}$$

Therefore low-impedance cables tend to have larger transfer admittances, but the effect of the transfer admittance on terminal voltage tends to be greatest for cables terminated in high impedances because $J\ell Z_1$ is proportional to the terminating impedance Z_1.

III BRAIDED SHIELDS

A. Transfer Characteristics

The characteristics of a braided shield can be defined in terms of the radius a of the shield,* the number of carriers C, (belts of wires) in the braid; the picks, P (number of carrier crossings per unit length); the ends, N (number of wires in each carrier); and the wire diameter, d. A typical braid pattern is shown in Figure 5(a) and an enlarged illustration of one diamond-shaped section of the braid is shown in Figure 5(b). The pitch angle α of the weave is

$$\alpha = \tan^{-1}\left[\frac{4\pi aP}{C}\right] \tag{27}$$

and the coverage of one carrier of the braid is

$$F = \frac{PNd}{\sin\alpha} = \frac{Nd}{W}. \tag{28}$$

The transparency of the crossed carriers [as shown in Figure 5(b)] is determined from the area of the diamond-shaped holes between the wires and the total area of the shield. From Figure 5(b) the area of the diamond formed by the crossed carriers is

$$A_c = \frac{W^2}{\sin 2\alpha}. \tag{29}$$

---

*Throughout this note it is assumed that the shields are thin and the holes are small so that $a \gg d$ and $a \gg r_o$.

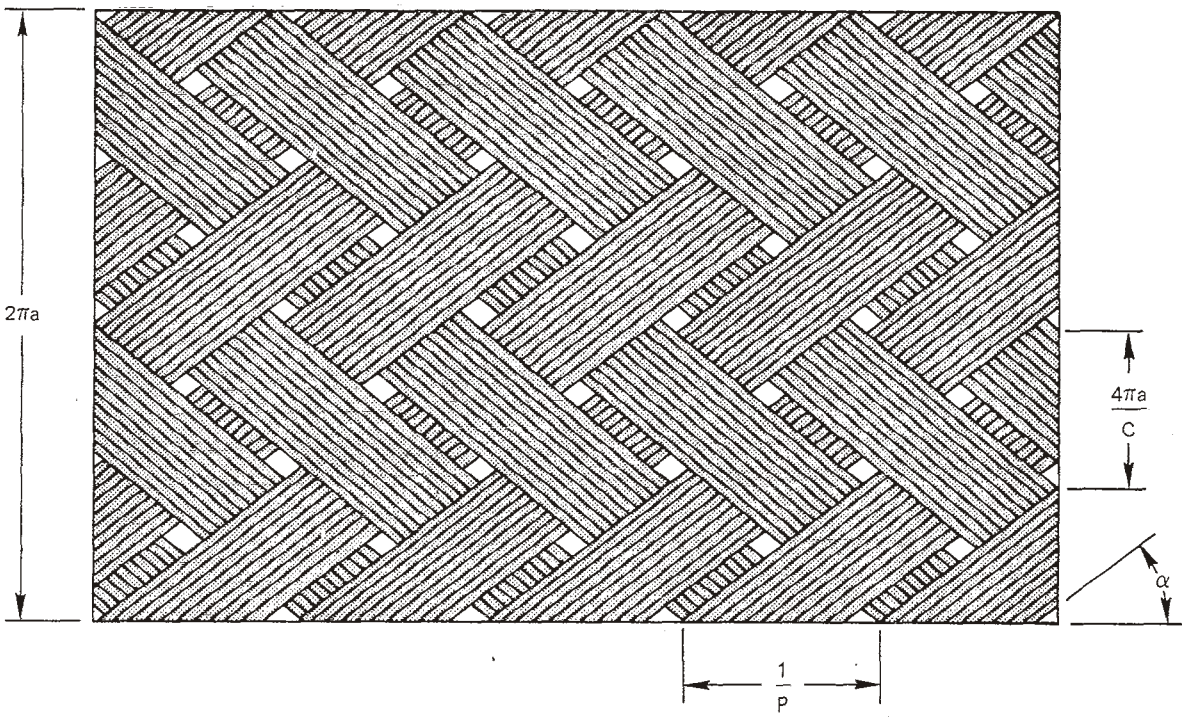

(a) BRAID PATTERN DEVELOPED ON A PLANE

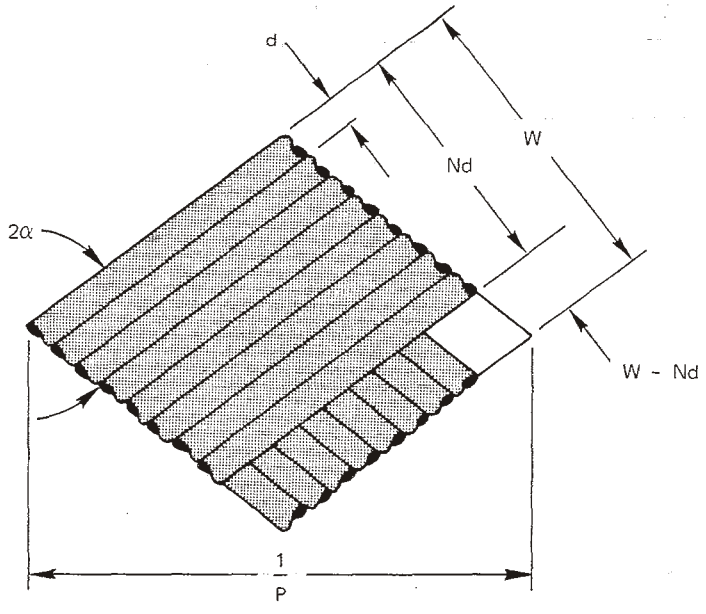

(b) ONE DIAMOND OF BRAID

TA-7995-292R

FIGURE 5 PROPERTIES OF A TYPICAL BRAIDED SHIELD

There is one diamond-shaped hole associated with each carrier-crossing. The area of each hole is

$$A_h = \frac{(W - Nd)^2}{\sin 2\alpha} \quad . \tag{30}$$

The shield transparency T is then

$$T = \frac{A_h}{A_c} = \frac{(W - Nd)^2}{W^2} \tag{31}$$

and the shield coverage is

$$K = 1 - \frac{A_h}{A_c} = \frac{2Nd}{W} - \left(\frac{Nd}{W}\right)^2 \tag{32}$$

$$= 2F - F^2 \quad .$$

The volume of metal in the braid is

$$v = NC\left(\frac{\pi d^2}{4}\right)\left(\frac{1}{\cos \alpha}\right) = \pi^2 adF \quad . \tag{33}$$

The number of holes per unit length in the braid is

$$\upsilon = PC = \frac{4\pi a \sin \alpha \cos \alpha}{N^2 d^2} F^2 \tag{34}$$

and each hole is a diamond whose longitudinal axis is

$$\frac{W - Nd}{\sin \alpha} = \frac{1}{P} - \frac{Nd}{\sin \alpha} = \frac{(1 - F)\ Nd}{F \sin \alpha} \qquad (35)$$

and whose transverse axis is

$$\frac{W - Nd}{\cos \alpha} = \frac{\tan \alpha}{P} - \frac{Nd}{\cos \alpha} = \frac{(1 - F)\ Nd}{F \cos \alpha} \qquad (36)$$

If the pitch angle α is less than 45°, the major axis of the diamond-shaped holes is perpendicular to the magnetic field, and the diamond is oriented for minimum magnetic coupling through the hole. If the pitch angle α is greater than 45°, the major axis is parallel to the magnetic field, and the hole is oriented for maximum magnetic coupling.

The transfer impedance of the braided shield can now be approximated with the guidance of the perforated-tube results. The transfer impedance will consist of two components, one representing diffusion of electromagnetic energy through the metal and one representing penetration of the magnetic field through the diamond-shaped holes. The diffusion term may be approximated by assuming that each conductor of diameter d is essentially isolated from all other conductors (i.e., that the contact resistance between wires is large compared to the wire resistance) so that the dc resistance per unit length of each conductor is

$$R_c = \frac{4}{\pi d^2 \sigma \cos \alpha}$$

and the resistance per unit length of the shield is

$$R_o \approx \frac{R_c}{NC} = \frac{4}{\pi d^2 NC \sigma \cos \alpha} = \frac{1}{\pi^2 ad \sigma F \cos^2 \alpha} \qquad (37)$$

The variation of this low-frequency diffusion term with frequency may be approximated by assuming that it behaves in the same manner as the diffusion term for the perforated shield of wall thickness d. Thus the approximate diffusion term for the braided shield will be

$$Z_d \approx \frac{4}{\pi d^2 \, NC \, \sigma \cos \alpha} \left(\frac{\gamma d}{\sinh \gamma d} \right) . \tag{38}$$

By analogy with the perforated shield we determine that the mutual inductance term for υ holes/m will be

$$M_{12} = \upsilon \frac{\mu_o m}{4\pi^2 a^2} \tag{39}$$

where m is the magnetic polarizability of the diamond-shaped hole and υ is the hole density given in Eq. (34) above. Although the polarizability of a diamond-shaped hole is not readily available from the literature, it can be determined experimentally using electrolytic-tank techniques.[4] Data for similar shapes, such as ellipses and slots with semicircular ends (see Figure 6) suggest that the polarizability of the diamond-shaped hole can be represented by the polarizability of an equivalent elliptical hole.[5] The magnetic polarizability of the elliptical hole has been derived in closed form for the magnetic field parallel to either axis of the ellipse. For an ellipse of eccentricity $e = \left[1 - (w/\ell)^2\right]^{1/2}$, where ℓ is the major axis and w is the minor axis, the magnetic polarizability is[4]

$$m_\ell = \frac{\pi \ell^3}{24} \left(\frac{e^2}{K(e) - E(e)} \right) \tag{40}$$

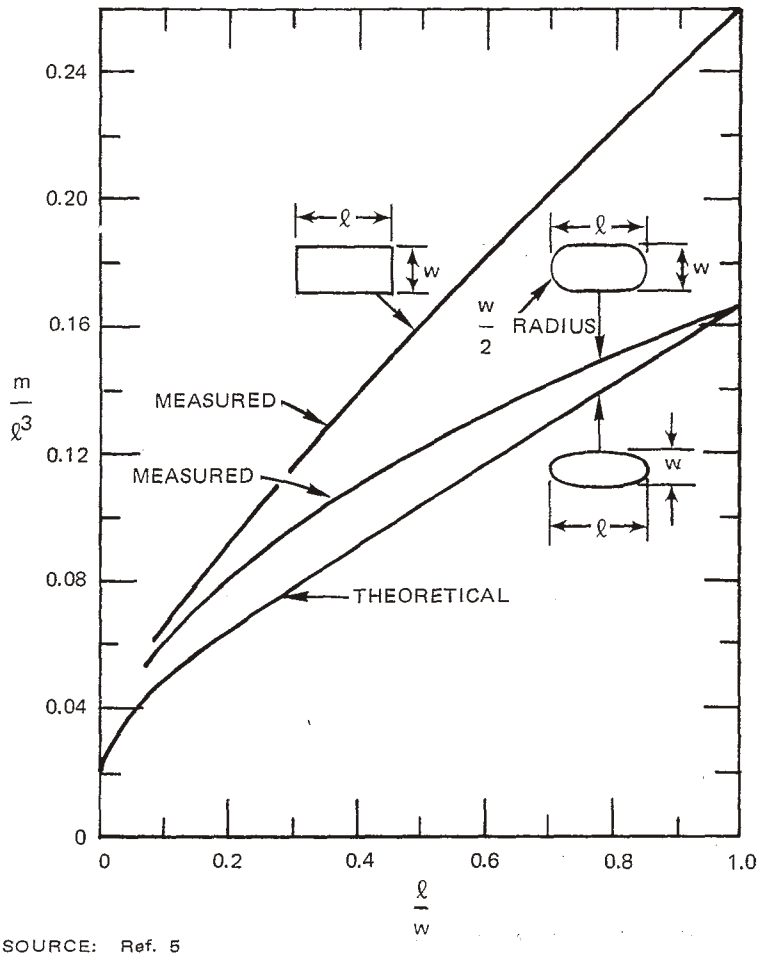

SOURCE: Ref. 5

TA-7995-222

FIGURE 6 MAGNETIC POLARIZABILITIES OF RECTANGULAR, ROUNDED-END, AND ELLIPTICAL SLOTS (magnetic field parallel to major axis)

for the magnetic field parallel to the major axis, and

$$m_w = \frac{\pi \ell^3}{24} \left(\frac{(1 - e^2)\, e^2}{E(e) - (1 - e^2)\, K(e)} \right) \tag{41}$$

for the magnetic field parallel to the minor axis. K(e) and E(e) are the complete elliptic integrals of the first and second kind, respectively, defined by

$$K(e) = \int_0^{\pi/2} \frac{d\varphi}{\sqrt{1 - e^2 \sin^2 \varphi}} \tag{42}$$

$$E(e) = \int_0^{\pi/2} \sqrt{1 - e^2 \sin^2 \varphi}\, d\varphi \quad . \tag{43}$$

Similarly the mutual capacitance between the internal conductor and the shield current-return conductor outside the shield is

$$C_{12} = \upsilon \frac{pC_1C_2}{4\pi a^2 \epsilon_o}, \tag{44}$$

where the electric polarizability of the ellipse is

$$p = \frac{\pi \ell^3}{24} \frac{1 - e^2}{E(e)} \quad . \tag{45}$$

Using the premise that the rhombic holes in a braided-shield pattern can be simulated by ellipses having similar major and minor axes, we obtain, for the mutual coupling associated with the holes,

$$\left.\begin{aligned} M_{12} &\approx \frac{\pi\mu_o}{6C} (1-K)^{3/2} \quad \frac{e^2}{E(e) - (1-e^2) K(e)} \quad \alpha < 45° \\ &\approx \frac{\pi\mu_o}{6C} (1-K)^{3/2} \quad \frac{e^2 / \sqrt{1-e^2}}{K(e) - E(e)} \quad \alpha > 45° \end{aligned}\right\} \tag{46}$$

and

$$C_{12} \approx \frac{\pi C_1 C_2}{6 \varepsilon C} (1-K)^{3/2} \frac{1}{E(e)} \qquad \alpha < 45°$$

$$\approx \frac{\pi C_1 C_2}{6 \varepsilon_o C} (1-K)^{3/2} \sqrt{\frac{1-e^2}{E(e)}} \qquad \alpha > 45° \qquad (47)$$

where K is the optical coverage, C is the number of carriers, and

$$e = \sqrt{1-\tan^2 \alpha} \qquad \alpha < 45°$$

$$= \sqrt{1-\cot^2 \alpha} \qquad \alpha > 45° \qquad (48)$$

The complete transfer impedance for the braided wire shield can then be written

$$Z_T \approx R_o \frac{\gamma d}{\sinh \gamma d} + j\omega M_{12} \qquad (49)$$

and the transfer admittance is $Y_T = j\omega C_{12}$. The high-frequency properties of the braided wire shield are thus determined by the coverage K, weave angle α (or excentricity e), and the number of carriers in the weave from Eqs. (46) and (47), and the low-frequency shielding properties are determined by the weave angle and shield material conductivity.

The variation of M_{12} and C_{12} with weave angle for constant coverage is shown in Figure 7. The mutual inductance per unit length increases rapidly with increasing weave angle, but the mutual capacitance C_{12} changes very little with weave angle. This is apparent in Figure 7 where shield radius, wire size, and number of ends has been fixed and the number of carriers is allowed to vary in such a manner that the coverage is constant.

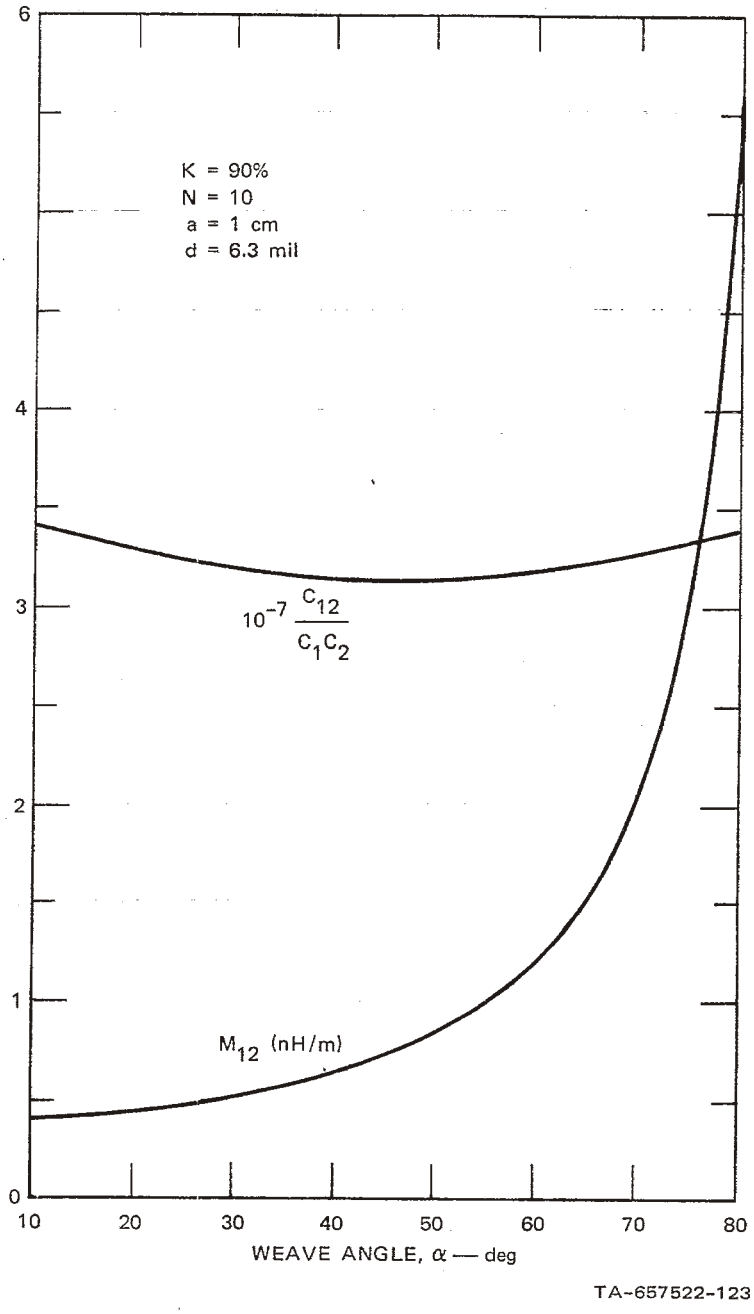

FIGURE 7 VARIATION OF MUTUAL INDUCTANCE AND MUTUAL CAPACITANCE WITH WEAVE ANGLE FOR CONSTANT COVERAGE

To illustrate the effect of M_{12} on the transfer impedance of a shield, the magnitude of the transfer function of Eq. (49) is plotted in Figure 8 as a function of frequency for a braided wire shield of 1 cm radius woven from 6.3 mil diameter copper wire. For comparison, the transfer impedance of a tubular shield 6.3 mils thick is shown as a dashed curve in Figure 8. As is often the case with braided shields, the leakage term $j\omega M_{12}$ dominates the transfer impedance at frequencies above about 1 MHz, while the diffusion term dominates below about 100 kHz. Note that this is true even with a tight weave (98 percent coverage). For a loose weave, the leakage may be observed to dominate the transfer impedance at frequencies below that at which the knee in the diffusion curve occurs.

B. Directional Effects in the Induced Signal

A comparison of the relative importance of the electric coupling associated with the transfer admittance and the magnetic coupling associated with the transfer impedance can be made by comparing the results for the short, lossless line terminated in its characteristic impedance Z_o. The total current from both coupling mechanisms for this case is, at $z = 0$ (the left end),

$$I(0) = \frac{I_o \ell}{2} \left(\frac{Z_T}{Z_o} + Y_T Z_{oe} \right) \tag{50}$$

and at $z = \ell$ (the right end) it is

$$I(\ell) = \frac{I_o \ell}{2} \left(\frac{Z_T}{Z_o} - Y_T Z_{oe} \right) \tag{51}$$

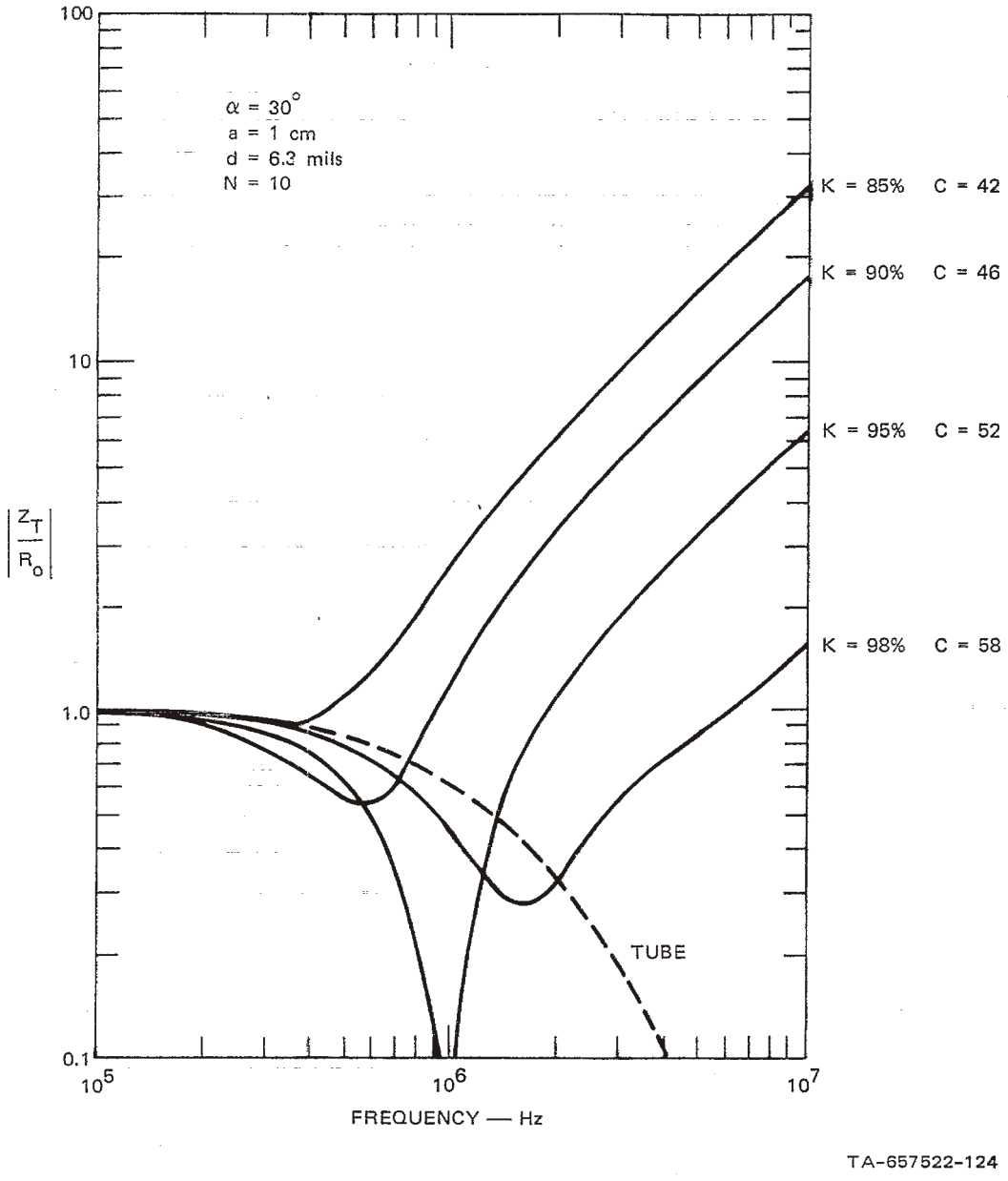

FIGURE 8 TRANSFER IMPEDANCE OF A BRAIDED-WIRE SHIELD

where ℓ is the length of the line, I_o is the shield current, and Z_{oe} is the characteristic impedance of the external shield curcuit. Because the electric and magnetic coupling are in phase for the negatively propagating components, the total coupled signal is greater for the matched load on one end (z = 0) than it is for the matched load at the other end. As is illustrated in Figure 9 for a short line, this directional effect is caused by the combination of a circulating current induced by the magnetic coupling with the shared current induced by the electric coupling. (This directional effect of coupling through small apertures, such as longitudinal slits, is the basis of some directional couplers.)

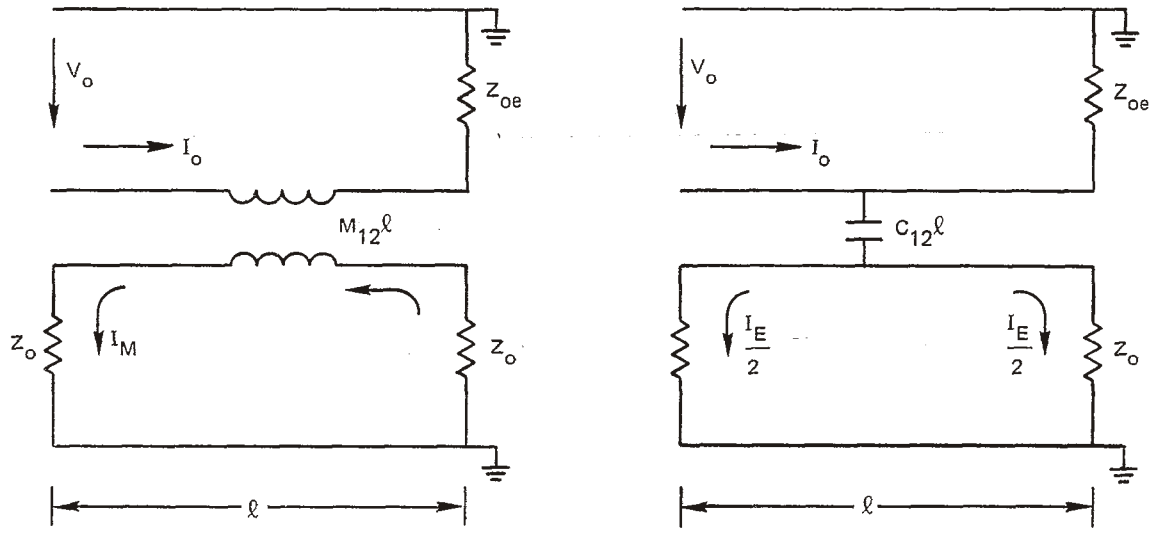

(a) MAGNETIC COUPLING (b) ELECTRIC COUPLING

TA-7995-291

FIGURE 9 COUPLING THROUGH A SHORT SEGMENT OF SHIELD THAT IS TERMINATED IN ITS CHARACTERISTIC IMPEDANCE INTERNALLY AND EXTERNALLY

The terms unique to magnetic and electric coupling in Eqs.(50) and (51) are Z_T/Z_o and $Y_T Z_{oe}$, respectively. If we take the ratio of these terms, we get

$$q = \frac{Z_T}{Z_o Z_{oe} Y_T} = \frac{M_{12}}{Z_o Z_{oe} C_{12}} \qquad (52)$$

at high frequencies where the transfer impedance is dominated by the mutual inductance M_{12}. From Eqs. (39) and (44),

$$\frac{M_{12}}{C_{12}} = \frac{\dfrac{\mu_o m}{4\pi^2 a^2}}{\dfrac{pC_1C_2}{4\pi^2 a^2 \varepsilon}} = \frac{\mu_o \varepsilon m}{C_1 C_2 p} \qquad (53)$$

where m and p are the magnetic and electric polarizabilities of the shield apertures, and C_1 and C_2 are the capacitance per unit length of the internal transmission line and the external transmission line,

Because $\mu_o \varepsilon = 1/v^2$, $C_1 = 1/vZ_o$ and $C_2 = 1/vZ_{oe}$, when the dielectric constant is the same inside and outside the shield the ratio of the magnetically induced current to the electrically induced current is

$$q = \frac{M_{12}}{Z_o Z_{oe} C_{12}} = \frac{m}{p} , \qquad (54)$$

the ratio of the magnetic and electric polarizabilities of the apertures in the shield. A plot of this ratio for the elliptic holes used to approximate the apertures in the braided wire shield is shown in Figure 10. From this plot, it is apparent that the magnetic coupling is larger than the electric coupling for all practical weave angles.

The ratio of the internal currents at the ends of the line is, from Eqs. (50), (51) and (54),

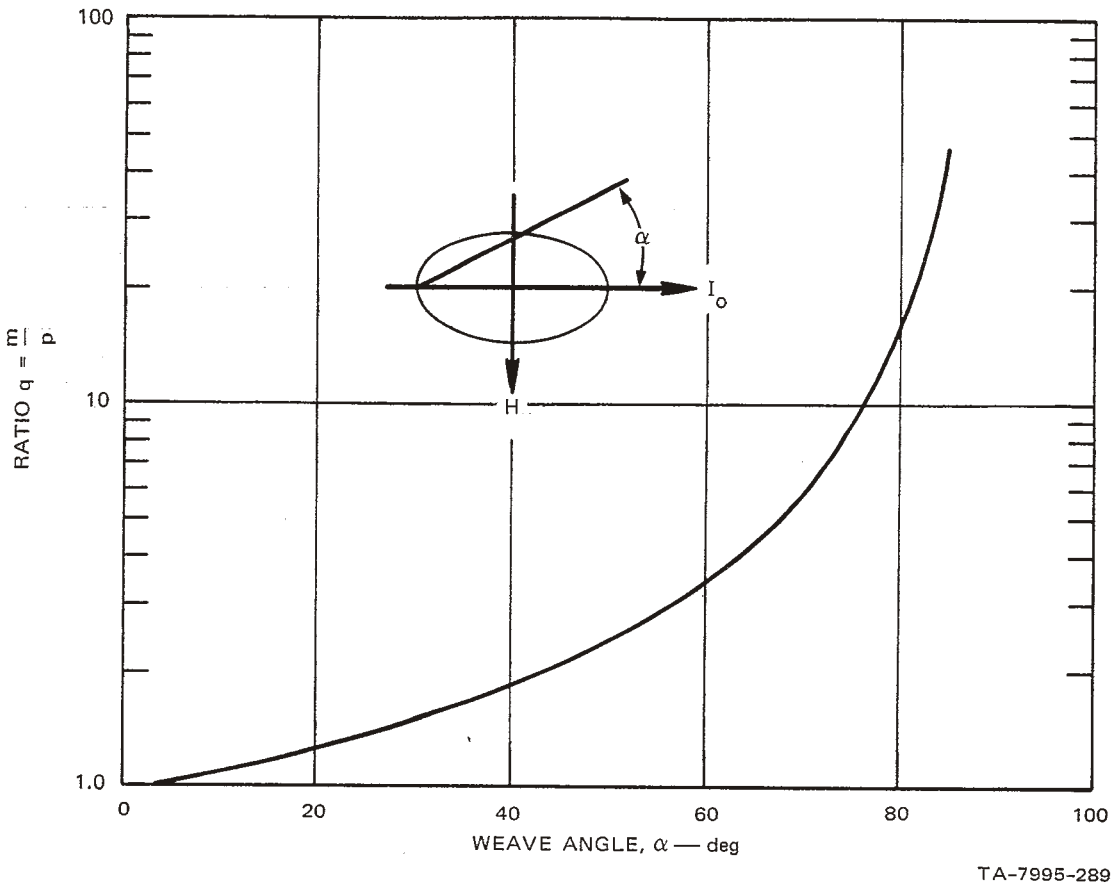

FIGURE 10 RATIO OF MAGNETIC POLARIZABILITY TO ELECTRIC POLARIZABILITY FOR ELLIPTICAL HOLES

$$\frac{I(\ell)}{I(0)} \approx \frac{m-p}{m+p} \quad . \tag{55}$$

This ratio is plotted in Figure 11 as a function of weave angle for the braided wire shield. As is apparent in Figure 11, this ratio is less than 0.1 for weave angles less than 20 degrees. This directional effect could, therefore, be very important in evaluating shielding effectiveness data measured under matched conditions.

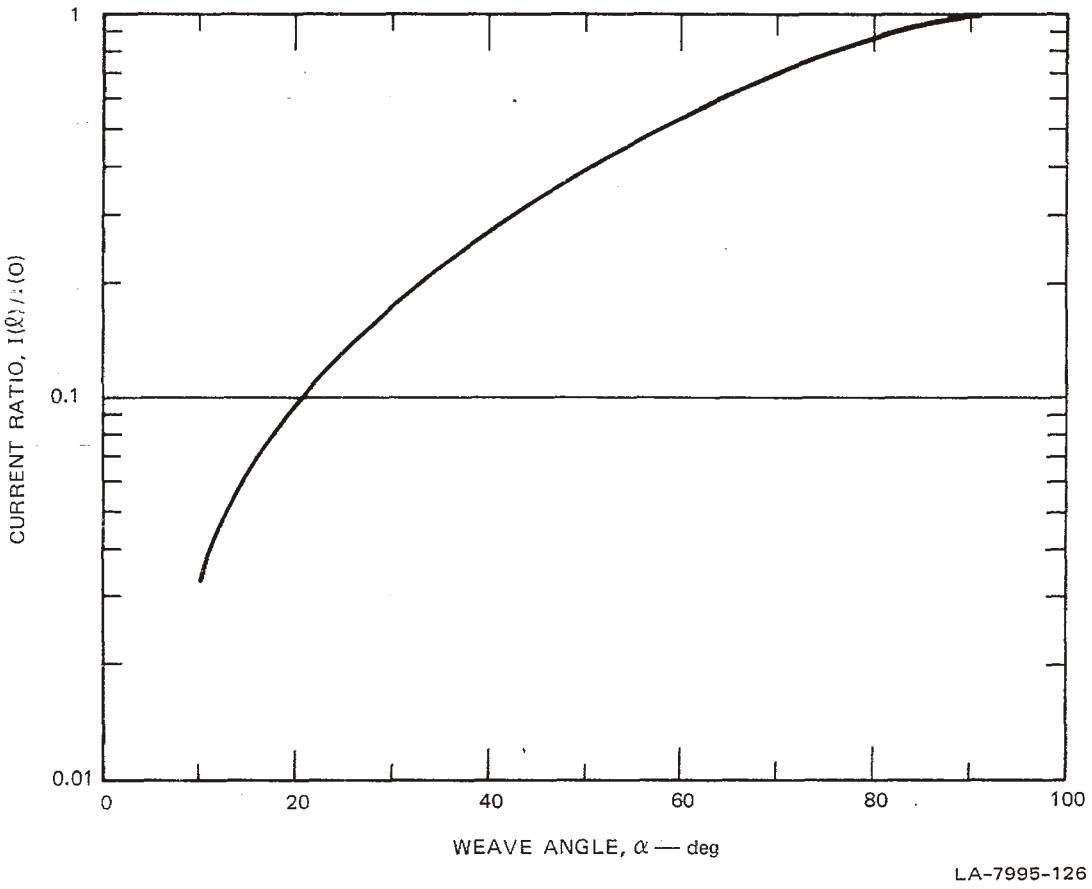

FIGURE 11 RATIO OF CURRENT AT RECEIVING TO CURRENT AT SENDING END DUE TO APERTURE COUPLING ALONE

IV DOUBLE-BRAIDED SHIELDS

A. Transfer Impedance

When two or more shields are used and the shields are connected together at electrically short intervals, the equivalent transfer impedance of the multiple-shield structure can be obtained by using an equivalent circuit model such as that shown in Figure 12. For two shields, this equivalent transfer impedance is

$$Z_T = \frac{E_2}{I_1} = \frac{Z_{T1} Z_{T2}}{Z_{S1} + Z_{S2} + j\omega L_{12}} \qquad (56)$$

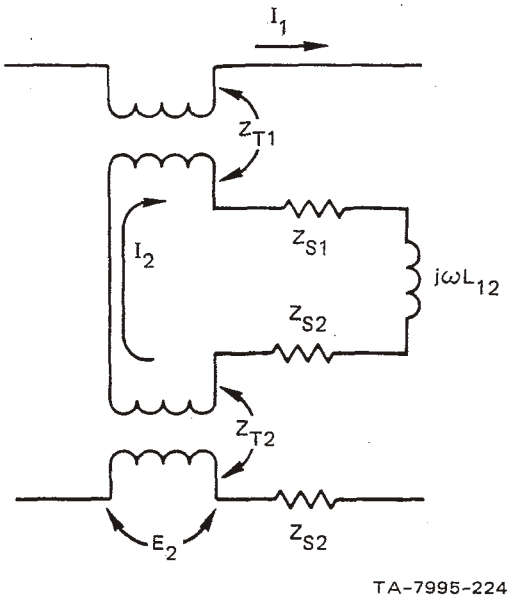

FIGURE 12 CIRCUIT MODEL FOR ANALYZING DOUBLE SHIELD

where

Z_{T1} = Transfer impedance of the first shield

Z_{T2} = Transfer impedance of the second shield

Z_{S1} = Internal impedance of the first shield

Z_{S2} = Internal impedance of the second shield

L_{12} = External inductance of gap between the shields.

The external inductance L_{12} between the shields is given by

$$L_{12} = \frac{\mu_o}{2\pi} \log \left(\frac{a_1}{a_2} \right) \tag{57}$$

where a_1 is the radius to the inside surface of the outer shield and a_2 is the radius to the outside surface of the inner shield. For thin tubular shields, the internal impedance is

$$Z_s \approx \frac{1}{2\pi a T \sigma} \gamma T \coth \gamma T \tag{58}$$

and by the same analogy used in arriving at Eq. (38), the internal impedance of a braided shield is approximately

$$Z_s \approx \frac{4}{\pi d^2 NC\sigma \cos\alpha} \gamma d \coth \gamma d \quad . \tag{59}$$

Normalizing the internal and transfer impedances to the dc resistance of the shield, we obtain

$$\frac{Z_s}{R_o} = \gamma d \coth \gamma d \tag{60}$$

and

$$\frac{Z_T}{R_o} = \frac{\gamma d}{\sinh \gamma d} + j \frac{\omega M}{R_o} \quad . \tag{61}$$

The equivalent transfer impedance of two braided shields is thus

$$Z_T = \frac{R_{o1} R_{o2} \left(\frac{\gamma_1 d_1}{\sinh \gamma_1 d_1} + j\omega \frac{M_1}{R_{o1}} \right) \left(\frac{\gamma_2 d_2}{\sinh \gamma_2 d_2} + j\omega \frac{M_2}{R_{o2}} \right)}{R_{o1} \gamma_1 d_1 \coth \gamma_1 d_1 + R_{o2} \gamma_2 d_2 \coth \gamma_2 d_2 + j\omega L_{12}} \quad . \tag{62}$$

This expression may be considerably simplified in two frequency ranges. When $|\gamma d| \ll 1$ (low frequencies) for both shields, $\gamma d / \sinh \gamma d \approx \gamma d \coth \gamma d \approx 1$, and in this frequency range both $j\omega M$ and $j\omega L$ are usually small compared to R_o (unless the braid is extremely transparent), so that

$$Z_T \approx \frac{R_{o1} R_{o2}}{R_{o1} + R_{o2}} \quad \text{(low frequencies)} \quad . \tag{63}$$

At high frequencies, such that ωM and ωL are much larger than the diffusion terms and $\omega L_{12} \gg Z_{s1}, Z_{s2}$,

$$Z_T \approx j\omega \frac{M_1 M_2}{L_{12}} \quad \text{(high frequencies)} \quad . \tag{64}$$

The frequency ranges where these approximations are valid are apparent from an examination of Figure 8. The low-frequency approximation applies in the region where the normalized transfer impedance of both shields is constant at a value of approximately 1.0, and the high-frequency approximation applies to the region where the transfer impedance is proportional to frequency. Because the gap inductance L_{12} is much greater than the mutual inductance $M_1 \approx M_2$, the high-frequency transfer impedance of the double-braided shield is much smaller than that of the single-braided shield. The low-frequency transfer impedance of the double braid differs by only a factor of 2 from that of the single braid, since the dc resistance of the double braid is roughly $\frac{1}{2}$ that of the single braid.

The analytical results for the double braid may be somewhat optimistic, since it is assumed that there is no direct coupling between the current in the outer shield and the interior conductors. This is tantamount to assuming that none of the magnetic field that penetrates the holes in the outer shield also penetrates holes in the inner shield. There will, or course, be some direct penetration through the holes in both shields, but the magnetic field penetrating both shields is expected to be a small fraction of the field penetrating the outer shield, particularly if there is significant space between the shields.

The improvement in high-frequency shielding effectiveness as measured by the ratio of the transfer impedances is

$$\frac{Z_T}{Z_{T2}} = \frac{j\omega \frac{M_1 M_2}{L_{12}}}{j\omega M_2} = \frac{M_1}{L_{12}} \quad . \tag{65}$$

Thus the greatest improvement is achieved (smallest value of M_1/L_{12}) when M_1 is small (low transparency, small weave angle) and L_{12} is large (large spacing between shields). Because a dielectric gap between the shields leads to resonant shield-to-shield transmission lines, which may be undesirable, an improved double-braided shield might be one that uses a layer of semiconducting plastic between the shields so that the inductance term L_{12} can be increased without introducing high-Q transmission-line resonances.

B. Mutual Capacitance

The effective mutual capacitance of the double shield can also be expressed in terms of the mutual capacitance between the shield return and the inner shield, the mutual capacitance between the outer shield and the core, the inductance L_{12}, and the number of places per unit length that the shields are connected together. To demonstrate this, let us break the problem into two parts, as suggested by Figure 13. First consider the two shields and the shield return path as illustrated in Figure 13(a). The shields are periodically shorted at υ_s points per unit length, and the mutual capacitance per unit length between the shield return (conductor 0) and the inner shield (conductor 2) is C_{02}. The current injected on the inner shield (conductor 2) by the external voltage V_e is $j\omega V_e C_{02}/\upsilon_s$. This current produces a voltage V_i between the shields at the injection point x_1 given by

$$V_i = \frac{j\omega V_e C_{02}}{\upsilon_s} \left[j\omega \frac{L_R L_L}{L_R + L_L} \right] \tag{66}$$

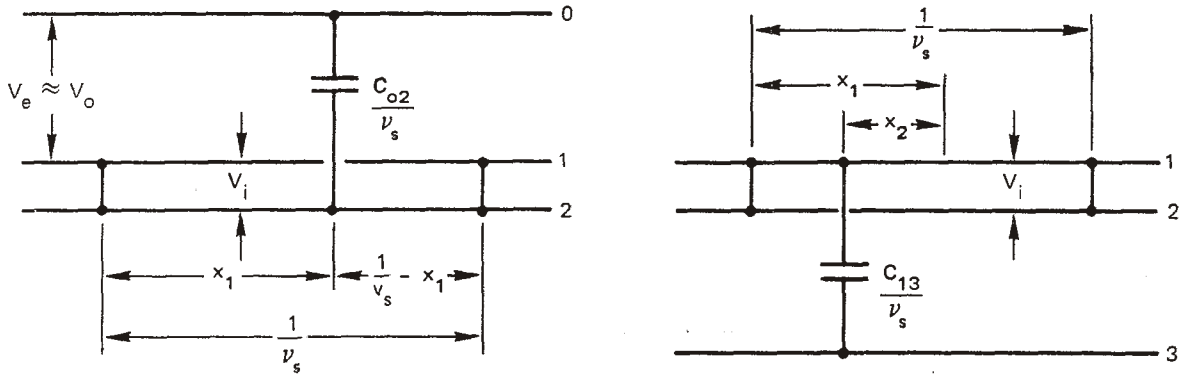

(a) SHIELDS WITH RETURN PATH

(b) SHIELDS WITH INNER CONDUCTOR

TA-7995-364

FIGURE 13 THE TWO PARTS OF THE ELECTRIC COUPLING PROBLEM FOR DOUBLE SHIELDS

where L_R is the inductance of the shorted section of transmission line to the right of the injection point x_1 and L_L is the inductance of the shorted line to the left. Since the inductance per unit length of the shield-to-shield transmission line is L_{12}, we have

$$L_R = L_{12}\left(\frac{1}{\upsilon_s} - x_1\right) \tag{67}$$

$$L_L = L_{12}(x_1) \tag{68}$$

and

$$\frac{L_R L_L}{L_R + L_L} = L_{12}\,\upsilon_s x_1\left(\frac{1}{\upsilon_s} - x_1\right) \quad . \tag{69}$$

The shield-to-shield voltage thus becomes

$$V_i = j\omega V_e C_{02}\left[j\omega L_{12}\, x_1\left(\frac{1}{\upsilon_s} - x_1\right)\right] \quad . \tag{70}$$

A hole in the inner shield located a random distance, x_2, from the hole in the outer shield [see Figure 13(b)] will be subjected to an excitation voltage $V_i(x_2)$. Because x_1, the location of the hole in the outer shield, is also assumed to be random, however, we will average V_i over all values of x_1. Thus we have

$$\overline{V_i} = j\omega V_e C_{02} (j\omega L_{12}) \upsilon_s \int_0^{\frac{1}{\upsilon_s}} x_1 \left(\frac{1}{\upsilon_s} - x_1 \right) dx_1$$

$$= \frac{(j\omega)^2 C_{02} L_{12} V_e}{6 \upsilon_s^2} \quad . \tag{71}$$

Referring now to Figure 13(b), the current per unit length injected on the core (conductor 3) by the voltage V_i is, on the average,

$$J = j\omega \frac{C_{13}}{\upsilon_s} \overline{V_i} \upsilon_s \quad . \tag{72}$$

When the average shield-to-shield voltage from Eq. (71) is substituted in Eq. (72), we obtain

$$J = (j\omega)^3 \frac{C_{13} C_{02} L_{12}}{6 \upsilon_s^2} V_e \quad . \tag{73}$$

Thus, the double shield can be replaced by a single shield whose mutual capacitance, C_{03}, is given by

$$C_{03} = (j\omega)^2 \frac{C_{13} C_{02} L_{12}}{6 \upsilon_s^2} \quad . \tag{74}$$

By expressing the mutual inductances and capacitances in terms of the polarizabilities of the holes in the shields, and assuming uniform dielectric throughout, we obtain

$$\frac{M_{12}}{C_{03}} = \frac{6 \upsilon_s^2}{(j\omega)^2 C_1 C_2} \frac{m_1 m_2}{p_1 p_2} \tag{75}$$

where C_1 is the capacitance per unit length between the outer shield and the return path and C_2 is the capacitance per unit length between the core and the inner shield. If the coefficient

$$\frac{6 \upsilon_s^2}{(j\omega)^2 C_1 C_2}$$

is less than 1, the ratio M/C for the double shield (i.e., the ratio of magnetic coupling to electric coupling) will be smaller than M/C for the single shield. Since $\upsilon_s \approx \upsilon \approx 1.5 \times 10^4 \ m^{-1}$ for the 1-cm-radius double-braided shield, and since $\sqrt{C_1 C_2} \approx 100$ pF/m is a representative geometric mean capacitance, the coefficient will be less than 1 for radian frequencies

$$\omega \geq \sqrt{\frac{6 \upsilon_s^2}{C_1 C_2}} \approx 3.7 \times 10^{14} \quad . \tag{76}$$

Thus for all radio frequencies normally of interest, the equivalent mutual inductance of the double braid is the only important leakage term for shielded cables near a ground plane serving as the shield-current return path.

As was the case in the analysis of the mutual inductance, this analysis of the mutual capacitance neglects the direct coupling between the core conductors and the shield return that is represented by field lines that originate on the shield return and penetrate through the holes in both shields to terminate on the core conductors. The analysis above also presumes a randomness in the location of the holes and short circuits that does not really exist in braided wire shields. The location of the shorts relative to each other and the location of holes relative to each other in one shield is not random in these shields. The location of the holes in the inner shield relative to the location of the holes in the outer shield may be quite random, however, and some holes in both shields may be eliminated entirely by being covered by a patch of braid that acts as a short circuit between the shields. It should also be apparent that for the hole densities and short densities typical of two-layer braided-wire shields, the assumption that the inductance of the shorted segments of shield-to-shield transmission line can be accurately represented by Eqs. (67) and (68) must be made with some skepticism. The intent of the analysis leading to Eq. (74) however, was to obtain an order-of-magnitude estimate of the effect of electric coupling through the two-layered shield so that it could be evaluated in relation to the magnetic coupling; this has been done.

V CONCLUSIONS

The analysis of braided shields presented here illustrates the nature of electromagnetic penetration of the shields and permits the effects of

various shield parameters on the shielding effectiveness to be assessed. Although the analytical approach used here utilized some simplifying approximations in both the diffusion and direct penetration analyses, it is doubtful that a more rigorous approach that takes into account the circular cross section of the wires and the rhombic shape of the holes would be justified for cable-shielding analysis. The trends of the shield behavior demonstrated here will not be altered by the more rigorous analysis, and it will usually be more economical and more accurate to measure the transfer impedance of a shield than to calculate it from basic parameters. Only measurements of the shielding effectiveness can be relied on to properly account for all of the details of braided wire shield design and manufacture.

The trends evolving from the analysis of braided shields indicate that the high-frequency shielding effectiveness depends not only on the shield coverage, but also on the size of the holes contributing to the coverage (or transparency). Thus, a shield with a given coverage is more effective if it contains many small holes than if it contains a few large holes. In terms of the fabric of the braid, the shield woven of fine wire with a small angle of weave provides the most effective shield for a given amount of copper per unit length of shield. The shielding effectiveness of the double-braided shield is much better at high frequencies than is the single-braided shield of the same coverage if the inductance of the gap between the shields is large compared to the mutual inductance of either shield. However, if the gap inductance is very small, or if the mutual inductance is very large, the additional copper invested in the second shield might better be used in a tighter and less transparent single braid.

REFERENCES

1. H. Kaden, Wirbelströme und Schirmung in der Nachrichtentechnik (Springer-Verlag, Berlin, 1959).

2. N. Marcuvitz, Waveguide Handbook, MIT Rad. Lab. Series, Vol. 10 (McGraw-Hill Book Company, New York, N. Y., 1951).

3. H. A. Bethe, "Theory of Diffraction by Small Holes," Phys. Rev., Vol. 66, pp. 163-182 (October 1 and 15, 1944).

4. C. G. Montgomery, R. H. Dicke, and E. M. Purcell, Principles of Microwave Circuits, MIT Rad. Lab. Series, Vol. 8, pp. 176-179 (Mc Graw-Hill Book Co., Inc., New York, N. Y., 1948).

5. S. B. Cohn, "Determination of Aperture Parameters by Electrolytic-tank Measurements," Proc. IRE., Vol. 39, pp. 1416-1421 (November 1951).

6. S. A. Schelkunoff, "The Electromagnetic Theory of Coaxial Transmission Lines and Cylindrical Shields," Bell System Tech. J., Vol. 13, pp. 532-579 (October 1934).

RELATED INTERACTION NOTES

IN 8 E. F. Vance, "Internal Voltages and Currents in Complex Cables", June 1967.

IN 29 C. W. Harrison, Jr., "Radio-Frequency Shielding of Cables", September 1961.

IN 30 R. W. P. King and C. W. Harrison, Jr., "Cylindrical Shields", March 1961.

IN 89 K. S. H. Lee, "Shields with Periodic Apertures", January 1972.

IN 90 R. W. Latham, "An Approach to Certain Cable Shielding Calculations", January 1972.

IN 104 C. D. Taylor and C. W. Harrison, Jr., "On the Excitation of a Coaxial Line Through a Small Aperture in the Outer Sheath", January 1972.

IN 118 R. W. Latham, "Small Holes in Cable Shields", September 1972.

IN 124 S. Frankel, "Terminal Response of Braided-Wire Cables to External Monochromatic Electromagnetic Fields", August 1972.

IN 132 K. S. H. Lee and C. Baum, "Application of Model Analysis to Braided-Shield Cables", January 1973.

IN 133 K. F. Casey, "Induced Currents on a Cable Shielded by Two Unidirectionally-conducting Shells", May 1973.